

Associated transverse energy in hadronic jet production

G. Marchesini

Dipartimento di Fisica, Università di Parma, Istituto Nazionale di Fisica Nucleare, Gruppo Collegato di Parma, Parma, Italy and Institute for Theoretical Physics, University of California, Santa Barbara, California 93106

B. R. Webber

Cavendish Laboratory, Department of Physics, University of Cambridge, Madingley Road, Cambridge CB3 0HE, United Kingdom and Institute for Theoretical Physics, University of California, Santa Barbara, California 93106

(Received 13 June 1988)

We present a theoretical study of the “pedestal height” in hadronic jet production, i.e., the mean transverse energy per unit of rapidity $\langle \omega_T^{\text{ped}} \rangle$ accompanying a high-transverse-energy jet. We find that perturbative QCD, supplemented by a Monte Carlo estimate of higher-order corrections and a soft underlying event structure similar to that of minimum-bias collisions, can account for the observed pedestal height and its dependence on jet transverse energy. We propose a way of separating the hard pedestal contribution from that of the underlying event by measuring the quantity $\langle \omega_T^{\text{dif}} \rangle$, which is one-half the absolute difference of the pedestal heights on the two sides of the jet. This quantity is dominated by the hard QCD component, whereas $\langle \omega_T^{\text{min}} \rangle = \langle \omega_T^{\text{ped}} \rangle - \langle \omega_T^{\text{dif}} \rangle$ is dominated by the soft underlying event. We also discuss the differential distribution of pedestal height and the charged multiplicity in the pedestal.

I. INTRODUCTION

An old prediction of perturbative QCD is the emergence of jets with large transverse energy in high-energy hadron collisions. Recent developments in the analysis of the theory now permit the prediction not only of the shape of the jet, i.e., the structure of the radiation emitted around the jet axis, but also of the structure of the radiation emitted outside the jet cone. These new theoretical results¹⁻³ are based on the resummation of all leading infrared singular contributions. In this way one finds that soft-gluon interference gives rise to the property of coherence for the QCD radiation.

In this respect the structure of the QCD radiation emitted outside the jet cone is of special interest. Since sizable interference takes place in this region, the distributions are particularly sensitive to the property of coherence both in the QCD cascades of timelike and spacelike partons, and in the matrix elements of the QCD hard subprocesses.

However, in hadron collisions the radiation outside the jet cone also has a component originating from the low- p_t interaction involving the spectator partons, which we shall call the *soft underlying event*. This interaction cannot be described by perturbative QCD. Therefore in order to be able to perform a clear analysis of the radiation in this phase-space region one should be able to disentangle the two contributions. In particular one can attempt to identify quantities which are most sensitive either to the hard perturbative or to the soft underlying components. One would then be able not only to perform a direct analysis of features related to perturbative QCD, but also to obtain, at the same time, phenomenological constraints on models for the soft underlying event.

Various data on the radiation emitted outside the jet cone are available.^{4,5} The quantity⁵ on which we shall focus our attention in this paper is the “pedestal transverse energy” $\langle \omega_T^{\text{ped}} \rangle$ for a jet of given transverse energy.

To define this quantity consider Fig. 1 in which we schematically represent $dE_T/d\eta$, the transverse-energy distribution integrated over the azimuthal angle ϕ on the same side of the jet axis ($|\Delta\phi| \leq \pi/2$). $\Delta\eta$ is the difference in (pseudo)rapidity ($\eta = -\ln \tan \frac{1}{2}\theta$) with respect to the jet axis. One then defines

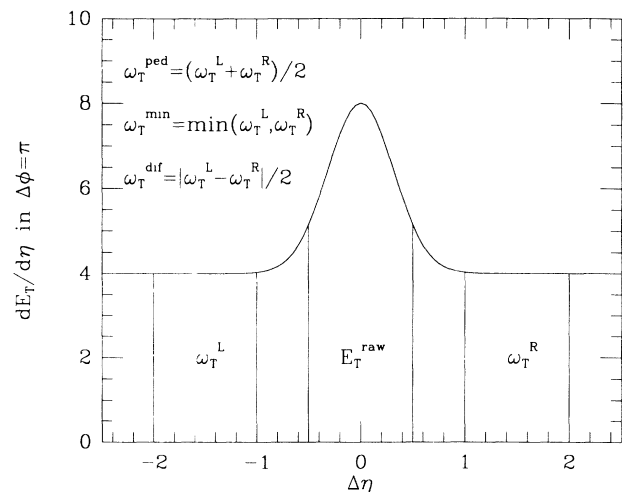


FIG. 1. Definition of the pedestal height and related quantities.

$$\omega_T^{\text{ped}} = \frac{1}{2}(\omega_T^L + \omega_T^R), \quad (1)$$

where, as indicated in Fig. 1, ω_T^L and ω_T^R are the transverse energies in the rapidity intervals $1 < |\Delta\eta| < 2$ on the two sides. The quantity $\langle \omega_T^{\text{ped}} \rangle$ is thus the average transverse energy per unit of rapidity measured in the pedestal, 1.5 units of rapidity away from the jet axis. The integration over $|\Delta\phi| < \pi/2$ avoids contributions to $\langle \omega_T^{\text{ped}} \rangle$ from the recoiling jet.

This quantity has been measured by the UA1 Collaboration⁵ at the CERN $p\bar{p}$ Collider for $\sqrt{s} = 630$ GeV and has the following features. It increases from $\langle \omega_T^{\text{ped}} \rangle \simeq 2$ GeV to about 4 GeV as the jet transverse energy increases to 10 GeV, then remains around this value for transverse energies up to the maximum measured value of 60 GeV. An analogous trend is observed in a similar quantity measured by the UA2 Collaboration.⁴

The pedestal height has been discussed by Sjöstrand and van Zijl,⁶ who propose a multiple-interaction model for the soft underlying event which can account for the above features. We shall consider this quantity instead from the viewpoint of perturbative QCD, supplemented by a more conventional model of the underlying event.

First of all we observe that $\langle \omega_T^{\text{ped}} \rangle$ is an infrared finite quantity and therefore its leading contribution can be computed in perturbation theory from the $(2 \rightarrow 3)$ matrix elements.

It is clear that this perturbative result cannot be directly compared with the data since, as explained before, $\langle \omega_T^{\text{ped}} \rangle$ receives substantial contributions from hadrons generated in the soft underlying event. However the perturbative analysis suggests a way to identify a quantity which is most sensitive to the hard component described by perturbative QCD. Since to leading order in α_s only the $(2 \rightarrow 3)$ parton matrix elements contribute, one has that to this order ω_T^L and ω_T^R cannot both be different from zero. Therefore we introduce the quantity

$$\omega_T^{\text{dif}} = \frac{1}{2}|\omega_T^L - \omega_T^R|, \quad (2)$$

which, to leading order, coincides with ω_T^{ped} .

On the other hand, the soft underlying contribution to $\langle \omega_T^{\text{dif}} \rangle$ should be small, for the following reason. The underlying event is expected to be similar to a minimum-bias soft collision. It is well established⁷ that such collisions show strong positive long-range rapidity correlations. Thus the underlying contributions to ω_T^L and ω_T^R should be strongly correlated and they should cancel in the difference.

Conversely, the quantity

$$\omega_T^{\text{min}} = \min(\omega_T^L, \omega_T^R) = \omega_T^{\text{ped}} - \omega_T^{\text{dif}} \quad (3)$$

vanishes in lowest-order perturbation theory, while the correlations in the underlying event mean that its contributions to ω_T^{min} and ω_T^{ped} should be comparable. Therefore $\langle \omega_T^{\text{min}} \rangle$ should be much more sensitive to the soft underlying contribution than $\langle \omega_T^{\text{dif}} \rangle$.

Thus measurements of the two quantities $\langle \omega_T^{\text{dif}} \rangle$ and $\langle \omega_T^{\text{min}} \rangle$, which have not yet been performed, would be helpful in disentangling the hard perturbative and the soft underlying components, respectively.

Another effect one should estimate when comparing the leading perturbative calculation of $\langle \omega_T^{\text{ped}} \rangle$ with the data is the size of higher-order corrections. This can be done by considering the multiparton amplitudes in the leading collinear and infrared approximation, which has been found to give a reliable estimate of higher-order corrections for various quantities ranging from the multi-jet cross sections⁸ in e^+e^- annihilation to the p_t and E_T distributions in Drell-Yan processes.³

Finally, one has to estimate the size of the contribution to $\langle \omega_T^{\text{ped}} \rangle$ due to the hadronization of QCD partons.

In this paper we perform a detailed study of $\langle \omega_T^{\text{ped}} \rangle$, $\langle \omega_T^{\text{dif}} \rangle$, and $\langle \omega_T^{\text{min}} \rangle$ using a recently developed Monte Carlo program³ for simulating hard QCD processes, which correctly sums not only the leading collinear singularities but also the infrared ones, thus taking into account the coherence of QCD radiation. Schematically the simulation consists of three stages.

(1) The perturbative QCD stage, in which off-shell partons are emitted according to the rules resulting from the analysis of the leading collinear and infrared singularities of Feynman diagrams.

(2) A hadronization model in which color-singlet clusters of partons decay into hadrons. Recall that according to perturbative QCD results⁹ these color-singlet clusters typically have small masses, so the resulting hadron distributions are not dissimilar from the parton distributions obtained in the previous stage.

(3) A model for the underlying event, in which low- p_t hadrons are generated by a soft collision between the two color-singlet clusters containing the spectators. This model is based on the UA5 Monte Carlo simulation of minimum-bias events.¹⁰

Using the Monte Carlo program we have computed the contributions to $\langle \omega_T^{\text{ped}} \rangle$, $\langle \omega_T^{\text{dif}} \rangle$, and $\langle \omega_T^{\text{min}} \rangle$ coming from the various stages of the simulation. In this way we can independently estimate (i) the perturbative QCD contributions including those due to higher-order corrections, (ii) the contribution from the process of hadronization of QCD partons, and (iii) the contribution from the soft underlying event.

In Sec. II we report the leading-order perturbative results for $\langle \omega_T^{\text{ped}} \rangle$ at $\sqrt{s} = 630$ and 1800 GeV in $p\bar{p}$ collisions, for the full range of jet transverse energy. In Sec. III we present the Monte Carlo results, compare them with the UA1 data, report the prediction at Fermilab Tevatron Collider energies, and discuss in more detail the possibility of disentangling the hard from the soft underlying component. Finally, Sec. IV contains a summary and some concluding remarks.

II. LEADING-ORDER RESULTS

Consider hadrons A and B colliding at c.m. energy \sqrt{s} and emitting a hard jet of transverse energy E_T . The leading-order contribution to $\langle \omega_T^{\text{ped}} \rangle$ is given by the hard subprocesses ($ab \rightarrow 123$). If $f_A(x_a)$ and $f_B(x_b)$ represent the momentum fraction distributions of parton a and parton b in hadrons A and B at the scale E_T , the average pedestal transverse energy is given by

$$\langle \omega_T^{\text{ped}} \rangle \frac{d\sigma}{dE_T} = E_T \alpha_s^3(E_T) \frac{1}{4\pi s^2} \int \omega_T^2 d\omega_T d\phi d\eta_1 d\eta_2 d\eta_3 \frac{f_A(x_a)}{x_a} \frac{f_B(x_b)}{x_b} \sum_{P(123)} |M_{ab \rightarrow 123}|^2, \quad (4)$$

where parton 1 represents the trigger jet, emitted at zero azimuthal angle with transverse energy E_T and rapidity $|\eta_1| < 1.5$. Parton 2 represents the recoiling jet on the opposite side, with rapidity η_2 integrated over the full range. Parton 3 then provides the contribution to the pedestal, with transverse energy ω_T , azimuthal angle $|\phi| \leq \pi/2$, and rapidity η_3 in the range $1 < |\eta_3 - \eta_1| < 2$. Finally $|M_{ab \rightarrow 123}|^2$ are the spin- and color-averaged amplitudes squared for the subprocesses ($ab \rightarrow 123$), which are summed over the permutations $P(123)$ of the emitted partons. In $|M_{ab \rightarrow 123}|^2$ we have factored out the coupling constant to show explicitly the argument used for α_s .

To leading order in α_s , the jet-transverse-energy distribution in (4) is given by the subprocesses ($ab \rightarrow 12$)

$$\frac{d\sigma}{dE_T} = E_T \alpha_s^2(E_T) \frac{2\pi}{s^2} \int d\eta_1 d\eta_2 \frac{f_A(x_a)}{x_a} \frac{f_B(x_b)}{x_b} \sum_{P(12)} |M_{ab \rightarrow 12}|^2, \quad (5)$$

where as before parton 1 represents the trigger jet with rapidity $|\eta_1| < 1.5$ and parton 2 the recoiling jet with rapidity integrated over the full range. E_T is the transverse energy of both emitted partons.

In Fig. 2 we show $\langle \omega_T^{\text{ped}} \rangle$ as a function of E_T computed for $p\bar{p}$ collisions at $\sqrt{s} = 630$ and 1800 GeV. These results are obtained using the structure-function parametrizations of Duke and Owens¹¹ (set 1, $\Lambda = 0.2$ GeV). We note the following points.

(i) $\langle \omega_T^{\text{ped}} \rangle$ rises rapidly at low E_T , has a broad maximum, and vanishes linearly as E_T approaches the kinematical limit $\sqrt{s}/2$. To understand this, note that the phase space in (4) vanishes more rapidly than that in (5) by one power of $(\sqrt{s}/2 - E_T)$.

(ii) Apart from a small scaling violation due to the structure functions in (4) and (5), the maximum value reached by $\langle \omega_T^{\text{ped}} \rangle$ increases with s as $\alpha_s(E_T)\sqrt{s}$, with E_T around the value at which the maximum of $\langle \omega_T^{\text{ped}} \rangle$ occurs.

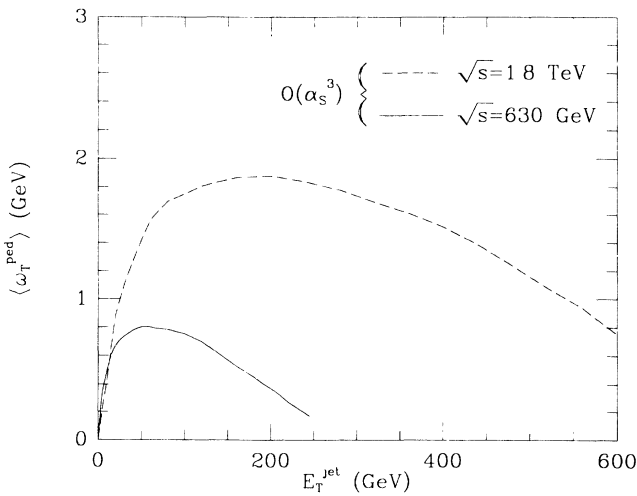


FIG. 2. Lowest-order perturbative QCD predictions of the mean pedestal height in $p\bar{p}$ collisions, as a function of the trigger jet energy.

(iii) The size of $\langle \omega_T^{\text{ped}} \rangle$, even at its maximum, is much smaller than the corresponding value of E_T . To understand this, note that, since the distribution $d\sigma/dE_T$ in (5) is a steeply falling function of E_T , it is more likely for the third parton to be emitted in the phase-space region opposite to the trigger jet, where it does not contribute to $\langle \omega_T^{\text{ped}} \rangle$.

(iv) The choice of E_T as the scale for the coupling constants in (4) is correct in an asymptotic calculation but might not be appropriate for a description at finite scale. In order to take into account the fact that the scale for the emission of the third parton is ω_T and not E_T one would replace $\alpha_s^3(E_T)$ in (4) by $\alpha_s^2(E_T)\alpha_s(\omega_T)$. This would enhance the value of $\langle \omega_T^{\text{ped}} \rangle$ by a factor of about 2 at CERN Collider energies. However, this goes beyond a leading-order calculation and therefore we show the lowest-order results with the scale taken to be E_T everywhere. But we must bear in mind when comparing with the Monte Carlo results in Sec. III that the parton branching scale used in the program is essentially the transverse energy of the radiated parton, i.e., ω_T for parton 3.

(v) By undoing the $\omega_T d\omega_T$ integration in (4) one also obtains the distribution of ω_T . For small ω_T this distribution has the infrared singular behavior $1/\omega_T$. Its explicit form will be reported and discussed later in connection with the higher-order corrections computed in the Monte Carlo simulation.

III. MONTE CARLO RESULTS

For the Monte Carlo study, the program of Ref. 3 was used to generate about 40 000 simulated $p\bar{p}$ events at $\sqrt{s} = 630$ GeV and about 20 000 at 1.8 TeV. The events were a mixture, in the expected proportions, of minimum-bias soft collisions and QCD jet events initiated by ($2 \rightarrow 2$) hard subprocesses with transverse energy per parton $E_T^{\text{hard}} > 3$ GeV. To reduce statistical fluctuations at high E_T , the jet events were generated with a flat input distribution in E_T^{hard} and reweighted appropriately. The Monte Carlo parameters were held fixed at the values given in Ref. 3.

The simulated events were analyzed using a simple

calorimeter simulation and a jet-finding algorithm¹² based on that of the UA1 experiment. We did not attempt to reproduce the details of the UA1 detector, but the quantities under investigation should not be very sensitive to such details.

The transverse energy of each event was registered in a 40×36 array of cells of size $\delta\eta\delta\phi = 0.2 \times 10^\circ$. The jet-finding algorithm searched for the cell with the highest remaining E_T greater than 1.5 GeV, then formed a jet from this and all surrounding cells with $E_T > 0.5$ GeV within $(\Delta\eta)^2 + (\Delta\phi)^2 < 1$. The jet energy and axis were defined by the vector sum of the positions of the jet cells, weighted by their energies. This gave the raw (i.e., uncorrected) jet transverse energy E_T^{raw} . The procedure was repeated until no more jets with $E_T^{\text{raw}} > 2.5$ GeV were found.

We checked that the resulting inclusive jet transverse energy distribution was in satisfactory agreement with experiment.^{5,13} The corresponding effective K factor, i.e., the final predicted jet cross section divided by the input lowest-order QCD value, decreased slowly from about 2.2 to 1.1 at high E_T , consistent with the mean value of about 1.5 suggested by experiment. This provides some additional reassurance that the Monte Carlo estimates of higher-order QCD correction, hadronization effects, and soft underlying contributions are reasonable.

For each jet found in the rapidity region $|\eta| < 1.5$, the associated values of ω_T^R, ω_T^L were obtained by summing the transverse energies of cells with $|\Delta\phi| < \pi/2$ and $-2 < \Delta\eta < -1, 1 < \Delta\eta < 2$, respectively, relative to the jet axis. The quantities $\omega_T^{\text{ped}}, \omega_T^{\text{dif}}$, and ω_T^{min} were then defined as in Fig. 1.

Three independent analyses along the above lines were performed for each simulated event: (i) a *parton* analysis based directly on the parton momenta generated in the perturbative phase of the simulation; (ii) a *hard* analysis using only the particles from the hard process, i.e., those resulting from the hadronization of the partons; and (iii) a *full* analysis using all final-state particles including those from the soft underlying event. In the full analysis, finite calorimetric energy resolution was taken into account, assuming electromagnetic and hadronic energy resolutions of $0.15/\sqrt{E}$ and $0.70/\sqrt{E}$, respectively (E in GeV). In fact, a fourth analysis, using all particles and assuming perfect energy resolution, was also carried out; the results are not shown because for the quantities under discussion they were essentially identical to those of the full analysis including resolution smearing.

The results on $\langle \omega_T^{\text{ped}} \rangle$, $\langle \omega_T^{\text{dif}} \rangle$, and $\langle \omega_T^{\text{min}} \rangle$, as functions of jet E_T^{raw} at $\sqrt{s} = 630$ GeV, are shown in Fig. 3. Figure 3(a) also shows the UA1 data¹⁵ on $\langle \omega_T^{\text{ped}} \rangle$. Taking into account the simplifications in the calorimeter simulation, the possible effects of different triggering conditions (minimum-bias trigger for the data at $E_T^{\text{raw}} < 20$ GeV, jet triggers above 30 GeV), and the absence of adjustable parameters, the agreement between the full simulation and the data seems satisfactory. The data suggest a slight enhancement in the range 15–40 GeV which is not present in the simulation. However, the rapid rise of $\langle \omega_T^{\text{ped}} \rangle$ to around 4 GeV for $E_T^{\text{raw}} \sim 10$ GeV, followed by a lack of strong dependence on jet energy up to 60 GeV,

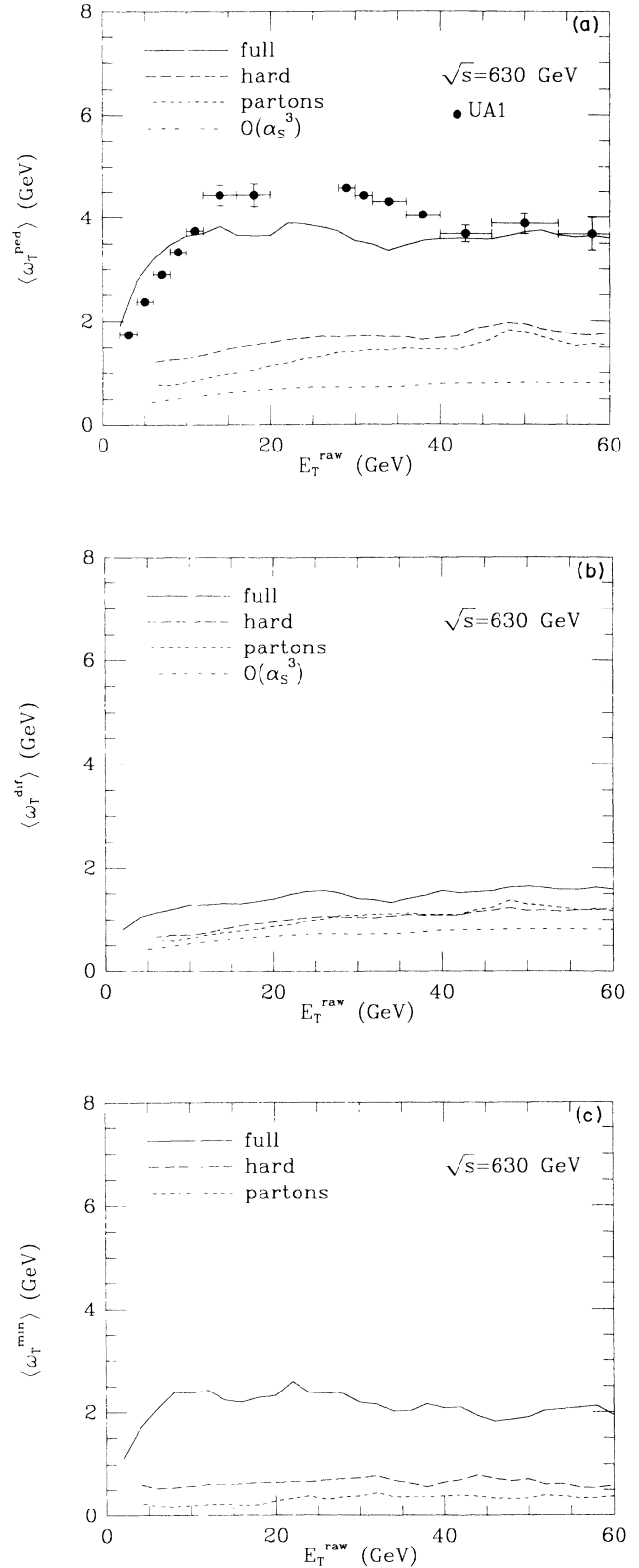


FIG. 3. Mean pedestal height and related quantities at the CERN $p\bar{p}$ Collider, as functions of observed jet transverse energy E_T^{raw} : (a) UA1 data (Ref. 5) and lowest-order and Monte Carlo predictions for $\langle \omega_T^{\text{ped}} \rangle$; (b) lowest-order and Monte Carlo predictions for $\langle \omega_T^{\text{dif}} \rangle$; (c) Monte Carlo predictions for $\langle \omega_T^{\text{min}} \rangle$.

are well reproduced.

In the region $E_T^{\text{raw}} \lesssim 10$ GeV, there are two types of events contributing to $\langle \omega_T^{\text{ped}} \rangle$: (i) genuine QCD jet events, which predominate above $E_T^{\text{raw}} \sim 5$ GeV and have roughly constant $\langle \omega_T^{\text{ped}} \rangle \sim 3.5$ GeV; (ii) soft events in which upward fluctuations in particle density are interpreted as “jets” by the jet-finding algorithm. The soft events predominate at $E_T^{\text{raw}} \lesssim 3$ GeV, where they have $\langle \omega_T^{\text{ped}} \rangle \sim 2$ GeV. At higher E_T^{raw} these events contribute a rapidly decreasing number of “jets,” for which $\langle \omega_T^{\text{ped}} \rangle$ tends to increase with E_T^{raw} owing to the long-range correlations in soft events. Thus when these events are combined with the genuine QCD jets the overall effect is a rapid rise in $\langle \omega_T^{\text{ped}} \rangle$, as observed.

Above 10 GeV, there is only genuine jet QCD production, and $\langle \omega_T^{\text{ped}} \rangle$ has the following components: (i) a parton-level contribution of 0.8–1.6 GeV, i.e., roughly twice the leading $\mathcal{O}(\alpha_s^3)$ prediction; (ii) a hadronization contribution of 0.2–0.5 GeV, leading to an overall hard contribution of 1.3–1.8 GeV; and (iii) an uncorrelated soft underlying contribution of around 2 GeV, producing an overall mean pedestal height of about 3.8 GeV, with little dependence on E_T^{raw} up to 60 GeV.

The factor of 2 enhancement in the hard pedestal at the parton level, relative to the lowest-order prediction, represents the Monte Carlo estimate of higher-order QCD corrections to this quantity. As explained in Sec. II, for the leading-order prediction we have taken α_s , to be evaluated at the scale E_T^{raw} , whereas a smaller scale of the order of ω_T , could be appropriate for one factor of α_s in (4). The Monte Carlo program actually uses such a scale and this accounts for most of the enhancement. As we shall discuss below, the lower effective scale is also reflected in the differential distribution of ω_T^{ped} at fixed E_T^{raw} .

Figure 3(b) shows how the contribution of the soft underlying event should be dramatically reduced, by a factor of about 4, if one studies $\langle \omega_T^{\text{dif}} \rangle$ instead of $\langle \omega_T^{\text{ped}} \rangle$. As explained in Sec. I this is because the strong long-range rapidity correlations observed in soft processes are expected to correlate ω_T^L and ω_T^R . The hard contribution, on the other hand, is reduced only by about 25%. We also observe that hadronization effects tend to cancel in $\langle \omega_T^{\text{dif}} \rangle$.

The situation is naturally just the opposite for $\langle \omega_T^{\text{min}} \rangle$. The parton-level contribution is small, less than 20%, and the predicted value of about 2.2 GeV is built almost entirely from the soft underlying and hadronization components.

At this point we should explain briefly how the Monte Carlo program generates the long-range rapidity correlations in the underlying event, which are important for the separation of this component. As mentioned earlier, the approach is essentially that of the UA5 simulation,¹⁰ which gives good agreement with the correlation data for minimum-bias events. The soft component of each event is assumed to consist of a number of low-mass low- p_t clusters, with a roughly uniform rapidity distribution. The multiplicity distribution of clusters is chosen to reproduce the observed minimum-bias charged-

multiplicity distribution, which is very broad, implying large global fluctuations in cluster multiplicity, i.e., large long-range correlations. Thus a large underlying contribution to ω_T^L most probably implies a large cluster multiplicity and hence also a large contribution to ω_T^R , as required for the soft component to cancel in $\langle \omega_T^{\text{dif}} \rangle$.

The predictions for $\sqrt{s} = 1.8$ TeV are shown in Fig. 4. (The greater fluctuations reflect the more limited statistics at this energy.) We expect a pedestal height of 5–6 GeV, with a clear rise in the range $20 < E_T^{\text{raw}} < 150$ GeV. The increase is almost entirely due to the hard component, since the soft contribution is practically independent of E_T^{raw} and varies only logarithmically with \sqrt{s} . A clear distinction should therefore be seen between the behavior of $\langle \omega_T^{\text{dif}} \rangle$, which is almost entirely hard and should rise by a factor of about 2 in this E_T^{raw} range, and $\langle \omega_T^{\text{min}} \rangle$, which is mainly soft and should show little increase with E_T^{raw} .

Figure 5 shows the E_T^{raw} dependence of the mean charged-particle multiplicity n_c in the pedestal at $\sqrt{s} = 630$ GeV. This quantity cannot be computed in fixed-order perturbation theory since it requires the resummation of infrared logarithms to all orders, which is performed by the Monte Carlo simulation. For the parton contribution, the quantity displayed is the quark (plus antiquark) multiplicity after splitting all gluons into $q\bar{q}$ pairs. As in the case of transverse energy we define $n_c^{\text{ped,dif}} = \frac{1}{2} |n_c^L \pm n_c^R|$. The results are very similar to those for ω_T , reflecting the fact that the charged/neutral particle ratio and mean transverse energy per particle do not depend strongly on E_T^{raw} . The same holds true at $\sqrt{s} = 1.8$ TeV (not shown).

As we have emphasized, an important feature of Figs. 3–5 is that the pedestal differences $\langle \omega_T^{\text{dif}} \rangle$ and $\langle n_c^{\text{dif}} \rangle$ provide a reliable guide to the hard contributions to $\langle \omega_T^{\text{ped}} \rangle$ and $\langle n_c^{\text{ped}} \rangle$ over a wide range of E_T^{raw} and \sqrt{s} . In more detail we may write

$$\begin{aligned} \langle \omega_T^{\text{dif}} \rangle_{\text{full}} &= \langle \omega_T^{\text{dif}} \rangle_{\text{hard}} + \langle \omega_T^{\text{dif}} \rangle_{\text{soft}} , \\ \langle \omega_T^{\text{ped}} \rangle_{\text{hard}} &= \langle \omega_T^{\text{dif}} \rangle_{\text{hard}} + \langle \omega_T^{\text{min}} \rangle_{\text{hard}} . \end{aligned} \quad (6)$$

Then $\langle \omega_T^{\text{min}} \rangle_{\text{hard}}$ and especially $\langle \omega_T^{\text{dif}} \rangle_{\text{soft}}$ are relatively small corrections, which moreover are roughly equal at present energies. As the c.m. energy increases, $\langle \omega_T^{\text{dif}} \rangle_{\text{soft}}$ should rise at most logarithmically, leading to even greater dominance of the hard contribution in $\langle \omega_T^{\text{dif}} \rangle$. Thus in Fig. 4(b) we see that $\langle \omega_T^{\text{dif}} \rangle_{\text{full}} \simeq \langle \omega_T^{\text{dif}} \rangle_{\text{hard}}$ is already quite a good approximation at $\sqrt{s} = 1.8$ TeV.

On the other hand, $\langle \omega_T^{\text{min}} \rangle_{\text{hard}}$, while remaining small compared with $\langle \omega_T^{\text{dif}} \rangle_{\text{hard}}$, should rise more rapidly than $\langle \omega_T^{\text{min}} \rangle_{\text{soft}}$, eventually predominating in $\langle \omega_T^{\text{min}} \rangle_{\text{full}}$. The trend in this direction may already be observed in Fig. 4(c).

Similar arguments to those above hold with ω_T replaced by n_c .

The predictions for the differential distribution of ω_T^{ped} at $\sqrt{s} = 630$ GeV for jets of transverse energy 60 GeV, including the lowest-order result obtained by undoing the $\omega_T d\omega_T$ integration in (4), are shown in Fig. 6. For sim-

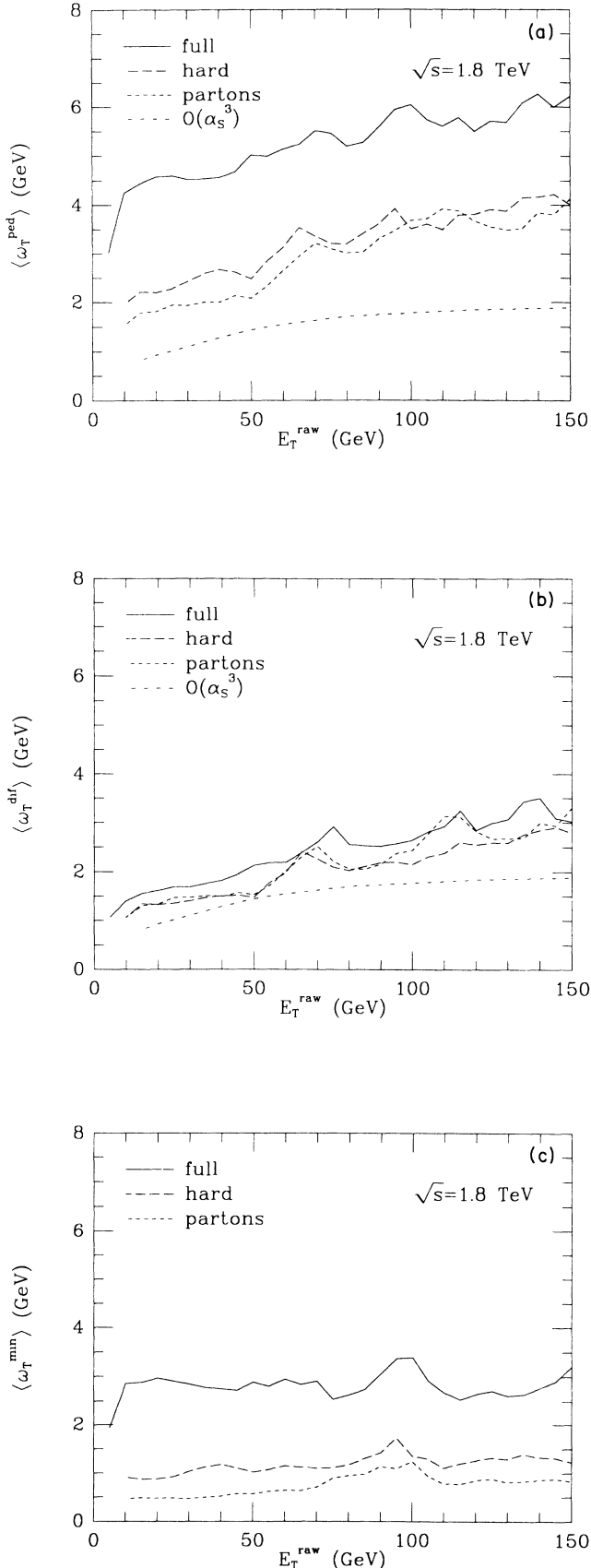


FIG. 4. As in Fig. 3 but for the Fermilab Tevatron Collider.

plicity, the Monte Carlo distributions in Figs. 6 and 7 were obtained by generating $(2 \rightarrow 2)$ hard subprocesses with $E_T^{\text{hard}} = E_T^{\text{jet}}$ and then taking the trigger jet to be the jet with the highest value of E_T^{raw} in each event. Thus E_T^{raw} was not precisely equal to E_T^{jet} but had a distribution peaked close to this value. The results look very similar throughout the range $20 < E_T^{\text{jet}} < 60$ GeV, so the distinction between E_T^{jet} and E_T^{raw} is not important here.

We see that the hard contribution in Fig. 6 converges to the lowest-order perturbative result at large ω_T^{ped} but is enhanced by a factor of 2–3 at lower ω_T^{ped} . It is this region that gives rise to the main nonleading corrections to $\langle \omega_T^{\text{ped}} \rangle$, due to the presence of powers of $\ln(E_T^{\text{raw}}/\omega_T^{\text{ped}})$ in higher orders. The main part of these corrections could be accounted for by choosing ω_T^{ped} instead of E_T^{raw} as the argument of one factor of α_s in (4), as discussed above.

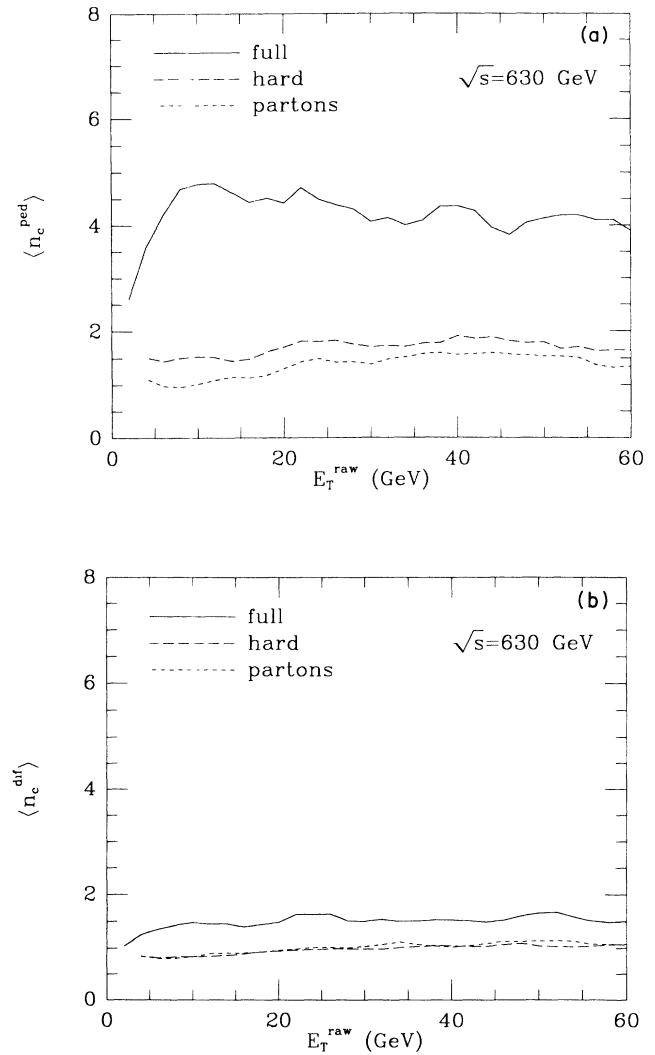


FIG. 5. Monte Carlo predictions for mean charged multiplicity per unit rapidity in the pedestal at the CERN $p\bar{p}$ Collider, as a function of observed jet transverse energy E_T^{raw} : (a) $\langle n_c^{\text{ped}} \rangle$; (b) $\langle n_c^{\text{dif}} \rangle$.

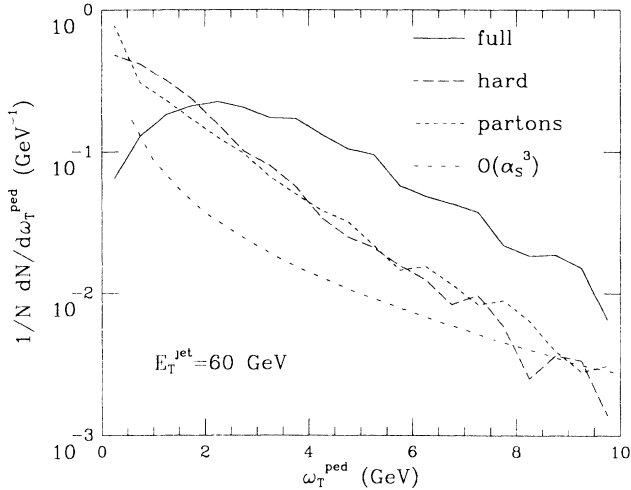


FIG. 6. Differential distribution of pedestal height for jets of transverse energy 60 GeV in $p\bar{p}$ collisions at $\sqrt{s} = 630$ GeV.

The Monte Carlo simulation uses such a scale and also sums various other large logarithms to all orders numerically.

The full distribution of ω_T^{ped} , after convolution with the soft underlying component, has a very different form from the hard part because the underlying contribution has no infrared singularity at $\omega_T^{\text{ped}}=0$. Again, however, we may exploit the expected long-range rapidity correlations in the underlying event to cancel most of its contribution by looking at ω_T^{dif} . As shown in Fig. 7, the resulting distribution should be dominated everywhere by the hard component, and at $\sqrt{s} = 630$ GeV the relation $(\omega_T^{\text{ped}})_{\text{hard}} \simeq (\omega_T^{\text{dif}})_{\text{full}}$, discussed above for the mean values only, actually holds for the distributions of these quantities.

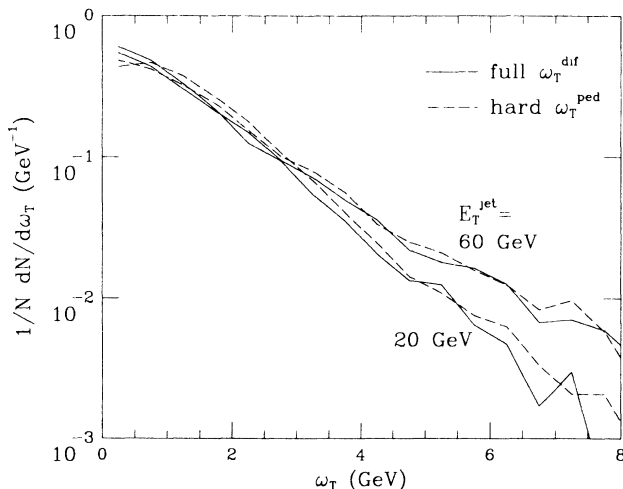


FIG. 7. Comparison between differential distributions of hard pedestal component and full pedestal difference ω_T^{dif} , for jets of transverse energies 20 and 60 GeV in $p\bar{p}$ collisions at $\sqrt{s} = 630$ GeV.

We should emphasize that the approximate equality between $(\omega_T^{\text{ped}})_{\text{hard}}$ and $(\omega_T^{\text{dif}})_{\text{full}}$ shown by the distributions in Fig. 7 does not hold quite so well on an event-to-event basis. The correction terms $(\omega_T^{\text{min}})_{\text{hard}}$ and $(\omega_T^{\text{dif}})_{\text{soft}}$ have approximately the same magnitudes and distributions at $\sqrt{s} = 630$ GeV but are almost completely uncorrelated. They contribute about 30% of $(\omega_T^{\text{ped}})_{\text{hard}}$ and $(\omega_T^{\text{dif}})_{\text{full}}$, respectively, so these quantities have a correlation coefficient of about 70%.

IV. CONCLUSIONS

In this paper we have shown that perturbative QCD, with higher-order corrections and soft contributions as estimated by the Monte Carlo simulation of Ref. 3, can account for the main features of the data on the mean pedestal height $\langle \omega_T^{\text{ped}} \rangle$ at the CERN $p\bar{p}$ Collider. Taking advantage of the factorized structure of the simulation (and of perturbative QCD) we have been able to study independently the various contributions to $\langle \omega_T^{\text{ped}} \rangle$. Roughly speaking we find that the total pedestal height of about 4 GeV is composed of (i) a lowest-order perturbative part of about 0.8 GeV, (ii) higher-order corrections (including rescaling the argument of α_s), about 0.8 GeV, (iii) hadronization contribution, about 0.4 GeV, and (iv) soft underlying event, about 2 GeV.

The model of the underlying event incorporated in the Monte Carlo program assumes that it is essentially just a minimum-basis soft event superimposed on the hard process. Since we can account for the data with this hypothesis we do not yet see a need for more complicated models such as that of Ref. 6.

We have also proposed a method for enhancing either the hard QCD component of the pedestal or the soft underlying one. The method involves measuring separately the two contributions $\langle \omega_T^{\text{dif}} \rangle$ and $\langle \omega_T^{\text{min}} \rangle$, in which the QCD and underlying components are enhanced, respectively.

Since only the sum of the two contributions has been measured so far, we have had to rely on the Monte Carlo simulation to test the method. Our study shows that it is quite efficient at CERN Collider energies: $\langle \omega_T^{\text{dif}} \rangle$ is dominated by the hard component and so one can test perturbative QCD more directly with this quantity. One may even study the hard component of the differential distribution of ω_T^{ped} in this way. The opposite happens for $\langle \omega_T^{\text{min}} \rangle = \langle \omega_T^{\text{ped}} \rangle - \langle \omega_T^{\text{dif}} \rangle$, which can thus be used to test different hypotheses about the soft underlying event. The only essential property that the underlying event must have in order to be enhanced in $\langle \omega_T^{\text{min}} \rangle$ is a strong long-range rapidity correlation.

We have studied the energy dependence of these quantities and in particular we have presented predictions at the energy of the Fermilab Tevatron Collider. The Monte Carlo simulation shows, as expected, that the enhancement of the hard component in $\langle \omega_T^{\text{dif}} \rangle$ is greater at higher energies, while the dominance of the underlying event in $\langle \omega_T^{\text{min}} \rangle$ becomes less strong.

The quantity $\langle \omega_T^{\text{ped}} \rangle$ is defined to suit the characteristics of the UA1 detector and may not be the best quantity to measure with other detectors. We should emphasize

therefore that the proposed method for separating the hard QCD and soft underlying components is simply based on the fact that the contribution of the former is asymmetrical while that of the latter is strongly correlated. Hence, one should be able to base the method on almost any pair of quantities involving the sum and difference of contributions in disjoint, comparable phase-space regions.

ACKNOWLEDGMENTS

It is a pleasure to acknowledge many helpful discussions on the topics of this paper with participants in the

QCD Program of the Institute for Theoretical Physics, especially M. Ciafaloni, S. D. Ellis, R. D. Field, F. E. Paige, and D. E. Soper. We are also grateful to T. Sjöstrand for constructive comments on our Monte Carlo program. This research was supported in part by the U.K. Science and Engineering Research Council and the Italian Ministero della Pubblica Istruzione and in part by the National Science Foundation under Grant No. PHY82-17853, supplemented by funds from the National Aeronautics and Space Administration, at the University of California at Santa Barbara. ara.

¹For a review, see L. A. Gribov, E. M. Levin, and M. G. Ryskin, *Phys. Rep.* **100**, 1 (1983); and A. Bassetto, M. Ciafaloni, and G. Marchesini, *ibid.* **100**, 201 (1983); see also S. Catani, M. Ciafaloni, and G. Marchesini, *Nucl. Phys.* **B264**, 588 (1986); B. R. Webber, *Annu. Rev. Nucl. Part. Sci.* **36**, 253 (1986); M. Ciafaloni, *Nucl. Phys.* **B296**, 249 (1987); R. K. Ellis, G. Marchesini, and B. R. Webber, *ibid.* **B286**, 643 (1987); Yu. L. Dokshitzer, V. A. Khoze, S. I. Troyan, and A. H. Mueller, *Rev. Mod. Phys.* **60**, 377 (1988).

²G. Marchesini and B. R. Webber, *Nucl. Phys.* **B238**, 1 (1984); B. R. Webber, *ibid.* **B238**, 492 (1984).

³G. Marchesini and B. R. Webber, *Nucl. Phys. B* (to be published).

⁴UA2 Collaboration, J. A. Appel *et al.*, *Phys. Lett.* **165B**, 441 (1985).

⁵UA1 Collaboration, C. Albajar *et al.*, Report No. CERN-

EP/88-29, 1988 (unpublished).

⁶T. Sjöstrand and M. van Zijl, *Phys. Rev. D* **36**, 2019 (1987).

⁷UA5 Collaboration, G. J. Alner *et al.*, *Phys. Rep.* **154**, 247 (1987).

⁸JADE Collaboration, W. Bartel *et al.*, *Z. Phys. C* **33**, 23 (1986).

⁹D. Amati and G. Veneziano, *Phys. Lett.* **83B**, 87 (1979); see also A. Bassetto, M. Ciafaloni, and G. Marchesini, *ibid.* **83B**, 207 (1979); G. Marchesini, L. Trentadue, and G. Veneziano, *Nucl. Phys.* **B181**, 335 (1981).

¹⁰UA5 Collaboration, G. J. Alner, *et al.*, *Nucl. Phys.* **B291**, 445 (1987).

¹¹D. W. Duke and J. F. Owens, *Phys. Rev. D* **30**, 49 (1984).

¹²F. E. Paige (private communication).

¹³UA2 Collaboration, J. A. Appel *et al.*, *Phys. Lett.* **160B**, 349 (1985).